

A Probabilistic Framework for Entire WSN Localization Using a Mobile Robot

F. Caballero^a L. Merino^b P. Gil^a I. Maza^a Aníbal Ollero^a

^aUniversity of Seville, Camino de los Descubrimientos s/n, 41092, Seville, Spain

^bPablo de Olavide University, Crta. de Utrera, km. 1, 41013, Seville, Spain

Abstract

This paper presents a new method for the localization of a Wireless Sensor Network (WSN) by means of collaboration with a robot within a Network Robot System (NRS). The method employs the signal strength as input, and has two steps: an initial estimation of the position of the nodes is obtained centrally by one robot and is based on particle filtering. It does not require any prior information about the position of the nodes. In the second stage, the nodes refine their position estimates employing a decentralized information filter. The paper shows how the method is able to recover the 3D position of the nodes, and is very suitable for WSN outdoor applications. The paper includes several implementation aspects and experimental results.

Key words: Wireless Sensor Network, Localization, Mobile Robots, Particle Filter, Information Filter

1 INTRODUCTION

In Network Robot Systems (NRS), a team of robots is expected to cooperate with sensors embedded in the environment for tasks like information gathering, tracking, surveillance, etc. Several different kinds of sensor networks can be expected, like surveillance cameras, RFID readers, etc. Latest advances in low-power electronics and wireless communication systems have made possible a new generation of devices able to communicate, sense environmental variables and even process this information, the Wireless Sensor Networks (WSNs). In WSNs, the sensors are cheap and the whole network can consist of hundreds of sensors. In addition, the

¹ This work is partially supported by the URUS project (IST-2006-045062) funded by the European Commission, and the AEROSSENS project (DPI-2005-02293) funded by the Spanish Government

27 recent commercialization of some of these devices has increased the applicability
28 and research efforts in this area.

29 Collaborative perception between robots and the sensor networks require to anchor
30 all the data gathered to the same reference frame. Therefore, the localization of
31 sensor nodes for sensor network deployment is an essential problem for NRS. It
32 can be also important for the network performance when geographic-based routing
33 methods are used. While most of the WSNs installed indoors are manually local-
34 ized, localization of all the nodes in outdoor applications is still an open problem
35 because GPS-based solutions are usually not viable due to the cost, the energy con-
36 sumption and the satellite visibility from each node.

37 This paper addresses the WSN localization problem in outdoor environments by
38 using a mobile robot. The paper describes a probabilistic framework where the
39 localization of an entire WSN can be estimated by analyzing the interactions of
40 a robot with the network. The approach takes advantage of the good localization
41 capabilities of the robot and its mobility to compute an initial estimation of the
42 node positions. The estimated position of the nodes could be used by the robot
43 to better plan actions for data recovering. Moreover, once an initial estimation is
44 obtained, a second localization stage is launched to refine the position of the nodes
45 in a distributed manner. The received signal strength from neighbor nodes is used
46 to improve their position employing a decentralized scheme based on Information
47 Filtering.

48 The paper is structured as follows. Firstly, the full approach is outlined in section
49 2. Section 3 details the proposed method to compute an initial estimation of the
50 position of the nodes. Then, a distributed technique for localization refinement is
51 described in section 4. Finally, some experimental results with a real network are
52 shown.

53 *1.1 Related work*

54 Localization of WSNs is an active field of research and some methods have been
55 proposed. Most of them [2,11,15] are based on a small and well distributed set of
56 nodes with known positions, called beacon-nodes. The position of these nodes is
57 computed by means of a positioning sensor such as GPS or active/passive posi-
58 tioning devices. Sometimes this position is simply pre-computed and stored in the
59 node. This information is propagated to the entire network and, finally, the radio
60 interface of the wireless nodes is used to estimate the distance to the beacon-nodes
61 which is used to estimate the localization of the nodes using triangulation, maxi-
62 mum bounding or other techniques.

63 A pre-calibrated relation between the Received Signal Strength Indication (*RSSI*)
64 provided by the communication circuitry and the distance is used to obtain a low-

65 accuracy estimation which worsens with the distance from the node to the beacon-
66 nodes, see [12]. Improvements in the radio interface to increase the directivity, as
67 in [19], or the inclusion of new features like time-of-flight have been proposed [18]
68 but, in general, they lead to a power consumption growth and to a radio coverage
69 reduction. In [9] time of arrival and direction of arrival are used to successfully
70 localize a wireless sensor network but a number of requirements such as sensor
71 node processor clock synchronization, special signal source devices and direction
72 of arrival are needed. Unfortunately, even having well localized beacon-nodes and a
73 reliable system to propagate this information, the results will be poor if the beacon-
74 nodes are not appropriately distributed in the network.

75 This paper proposes to use a mobile robot equipped with a DGPS device for WSN
76 calibration. A mobile node can substitute a set of fixed beacon-nodes. Some au-
77 thors have proposed the use of mobile robots for calibration of sensor networks.
78 For instance, in [1] the authors present a similar approach based on particle filters
79 for the calibration of a network of cameras. A particle filter is used to estimate the
80 pose of the cameras, and it employs as data the position on the image plane of a
81 localized robot. It also combines this with a Kalman Filter for position refinement.
82 However, results with only one camera are presented, and no distributed approach is
83 proposed. In [13], the authors consider the use of a mobile robot carrying a calibra-
84 tion pattern for the simultaneous localization, mapping and calibration of a indoors
85 network of cameras. There, a centralized Extended Kalman Filter is employed to
86 fuse all the information and the use of the artificial pattern allows to fully observe
87 the position of the robot relative to the camera.

88 A technique for WSN localization using mobile robots has been also presented
89 recently in [3]. The authors detail a technique based on potential fields that exploits
90 the position information of a team of Unmanned Aerial Vehicles (UAVs) to localize
91 the nodes. The concept underlying the approach is similar to ours, although the
92 solution adopted is different; moreover, an accurate range sensor is required for
93 computing the distance from the UAVs to the nodes. Here no special device for
94 distance computation is used.

95 **2 TECHNIQUE OVERVIEW**

96 The purpose of the presented technique is to localize all the nodes of the network by
97 using the information gathered by a mobile robot. The robot is able to communicate
98 with the WSN in order to obtain environmental information. These data are sent to
99 the robot by using a radio frequency stage that informs about the signal strength on
100 reception (the *RSSI* value).

101 The approach, outlined in Fig. 1, uses the received signal strength to estimate the
102 position of the emitter. The technique can be divided into two basic steps. Firstly,

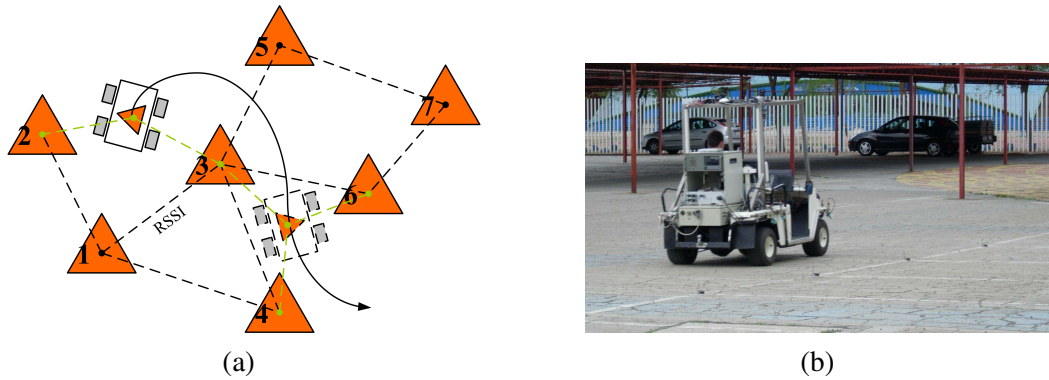


Fig. 1. (a): Scheme of the approach. The signal strength is used to estimate the position of the nodes of the network. The mobile robot computes centrally an initial estimation employing a separate Particle Filter per node. In the second step, a decentralized Information Filter integrates at each node information received from neighbor nodes and the robot. (b): An example, a ground robot (Romeo) driving through the network

103 a Particle Filter is used to process the *RSSI* value received from each node to com-
 104 pute an initial estimation of node locations in a static wireless network. The filter
 105 takes into account the uncertainty associated with the *RSSI* value and with the robot
 106 position (provided by a DGPS device) in order to optimally compute the position of
 107 the node. In the second step, the initial estimation of the position of the nodes (rep-
 108 resented by mean and standard deviation) is sent to them. A distributed Information
 109 Filter is implemented in each node in order to easily improve the localization using
 110 the signal strength received from other nodes of the network, including the mobile
 111 robot.

112 The following characteristics differentiate this technique from other approaches:

- 113 • A Bayes filter is employed for the estimation of the localization of the nodes. The
 114 estimated position of the nodes will be represented by a probability distribution.
 115 This allows to take into account the uncertainty on measures involved in the
 116 process, mainly the relationship between *RSSI* and distance.
- 117 • The mobile robot position is included in the localization process and integrated
 118 along time. It allows to reduce one of the endemic problems of the *RSSI*-based
 119 localization algorithms: the distortion induced by radio-frequency effects. The
 120 chance of measuring the *RSSI* at different robot positions and orientations per-
 121 mits automatic detection of outliers and, hence, an improvement in the distance
 122 computation.
- 123 • Once an initial solution is computed, the network is able to use the localization
 124 information of all the nodes, including the position of the robot, to improve the
 125 estimation. This increases the flexibility of the technique.
- 126 • There is no triangulation but an estimation process so that the algorithm can
 127 consider hypotheses in which the estimated position is spread over a certain area.

128 3 PARTICLE FILTER BASED NODES LOCALIZATION

129 3.1 Filter overview

130 The objective of the localization algorithm is to estimate the position of the nodes
131 of the network from the data provided by the node onboard the robot equipped with
132 DGPS. A separate filter is implemented per node. Then, the state to be estimated
133 consists of the position of each node $\mathbf{x} = (X \ Y \ Z)^T$. The information about the
134 state will be obtained from the set of measurements $\mathbf{z}_{1:k}$ received up to time k . This
135 set of measurements consists of pairs of *RSSI* and robot position values $\{\mathbf{x}_k^r, RSSI_k\}$
136 (the algorithm considers a moving robot, and thus the time subscript for the robot
137 position).

138 The method is based on Particle Filtering. This technique allows implementing re-
139 cursive Bayesian filtering by Monte Carlo sampling. The key idea is to represent
140 the posterior density at time k $p(\mathbf{x}_k|\mathbf{z}_{1:k})$ by a set of independent and identically
141 distributed (i.i.d.) random particles $\{\mathbf{x}_k^{(i)}\}$ according to the distribution. Each par-
142 ticle is accompanied by a weight $\omega_k^{(i)}$. Sequential observations and model-based
143 predictions will be used to update the weight and particles respectively. See [4] for
144 more details.

145 Particle Filters allow Bayesian estimation to be carried out approximately but in
146 a structured and iterative manner, that simplifies the implementation. In general,
147 it is very suitable for non-gaussian stochastic processes with non-linear dynamics
148 and very useful when the posterior $p(\mathbf{x}_k|\mathbf{z}_{1:k})$ has no parametric form or this form is
149 unknown. 3D localization of nodes with non prior information implies a completely
150 unknown posterior, so that Particle Filter seems to be a good solution to address the
151 node localization problem.

152 Although there are many possible implementations, in the proposed algorithm the
153 prior probability distribution $p(\mathbf{x}_0)$ is used as the importance (or proposal) distribu-
154 tion to draw the initial set of particles at time 0, i.e. $\mathbf{x}_0^{(i)} \sim p(\mathbf{x}_0)$. Then, these parti-
155 cles are recursively re-estimated following the algorithm shown in Algorithm 1.

156 Next subsections describes the main issues in the actual implementation of the al-
157 gorithm. As the likelihood function is the core of the algorithm, it is described first.
158 Then the updating step, the prior distribution, the prediction step and the resam-
159 pling procedure are detailed. Finally, some guidelines for computing the mean and
160 standard deviation in the filter are mentioned.

Algorithm 1 $\{\mathbf{x}_k^{(i)}, \omega_k^{(i)}; i = 1, \dots, L\} \leftarrow \text{Particle_filter}(\{\mathbf{x}_{k-1}^{(i)}, \omega_{k-1}^{(i)}; i = 1, \dots, L\}, \mathbf{z}_k = \{\mathbf{x}_k^r, RSSI_k\})$

- 1: **for** $i = 1$ to L **do**
- 2: sample $\mathbf{x}_k^{(i)} \sim p(\mathbf{x}_k | \mathbf{x}_{k-1}^{(i)})$
- 3: Compute $d_k^{(i)} = \|\mathbf{x}_k^{(i)} - \mathbf{x}_k^r\|$
- 4: Determine $\mu(d_k^{(i)})$ and $\sigma(d_k^{(i)})$
- 5: Update weight of particle i $\omega_k^{(i)} = p(RSSI_k | \mathbf{x}_k^{(i)}) \omega_{k-1}^{(i)}$ with $p(RSSI_k | \mathbf{x}_k^{(i)}) = \mathcal{N}(\mu(d_k^{(i)}), \sigma(d_k^{(i)}))$
- 6: **end for**
- 7: Normalize weights $\{\omega_t^{(i)}\}, i = 1, \dots, L$
- 8: Compute N_{eff}
- 9: **if** $N_{eff} < N_{th}$ **then**
- 10: Resample with replacement L particles from $\{\mathbf{x}_k^{(i)}, \omega_k^{(i)}; i = 1, \dots, L\}$, according to the weights $\omega_k^{(i)}$
- 11: **end if**

161 **3.2 The likelihood function**

162 The likelihood function $p(\mathbf{z}_k | \mathbf{x}_k)$ plays a very important role in the estimation pro-
 163 cess. In this case, this function expresses the probability of obtaining a given *RSSI*
 164 value on the node onboard the robot (at position \mathbf{x}_k^r) given the position of the emitter
 165 node \mathbf{x}_k .

166 Experimental results (Fig. 2) show that there exists a correlation between the dis-
 167 tance that separate both nodes and the *RSSI* value, although this correlation de-
 168 creases with the distance between the two nodes, transmitter and receiver. This is
 169 mainly caused by radio-frequency effects such as radio reflection, multi-path or
 170 antenna polarization.

171 The model used here considers that the conditional density $p(\mathbf{z}_k | \mathbf{x}_k)$ can be approx-
 172 imated as a Gaussian distribution for a given distance $d_k = \|\mathbf{x}_k - \mathbf{x}_k^r\|$ as follows:

$$RSSI_k = \mu(d_k) + \mathcal{N}(0, \sigma(d_k)) \quad (1)$$

173 where the functions $\mu(d_k)$ and $\sigma(d_k)$ are non-linear functions of the distance (which
 174 itself is a non-linear function of the state).

These functions are estimated offline from a training data set. A couple of nodes have been distanced from 0 to 30 meters and the *RSSI* has been recorded for each distance. This experiment has been repeated with several antenna polarizations. A least squares process was used to compute the $\mu(d_k)$ and $\sigma(d_k)$ functions that best

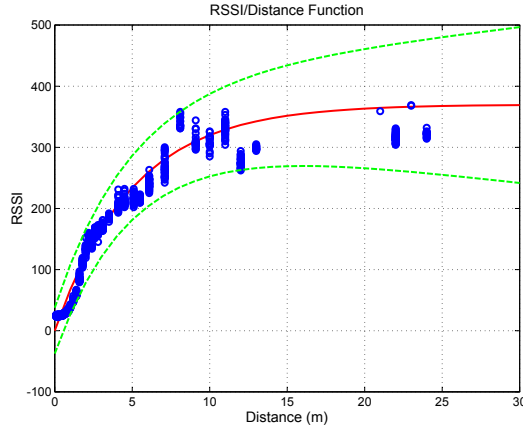


Fig. 2. RSSI-Distance functions, $\mu(d_k)$ and $\sigma(d_k)$. These functions relate the distance between two nodes and the RSSI received in mean and std. deviation. It has been experimentally computed using a large set of RSSI/distance couples. The RSSI representation is the one used in the Mica2 nodes, 0 is the maximum signal strength and 375 the minimum. Dots: A sub-set of the experimental set of data. Solid line: Estimated mean $\mu(d_k)$. Dashed lines: standard deviation confidence interval based on $\sigma(d_k)$.

fit the set of data. The computed equations are the following:

$$\mu(d_k) = 360 \cdot (1 - e^{-0.2 \cdot d_k}), \quad \sigma(d_k) = 2.11 \cdot d_k + 25.36 \quad (2)$$

175 These equations are also shown in Fig. 2. As expected, it can be seen that the
 176 standard deviation increases with the distance d_k .

177 Note that the empirical model defined by (1) and (2) consider not only the antenna
 178 properties, but also the filtering and data conversions carried out by the communica-
 179 tions circuitry. For that reason, the model does not match with the classic logarith-
 180 mic free space propagation equations. Nevertheless, the experiment data agree with
 181 those obtained in [14], where the authors also identify quasi-gaussian distributions
 182 in the relations RSSI/distance for a fixed distance.

183 This experiment is only carried out for a couple of nodes of the network. Unfor-
 184 tunately, the nodes on a WSN are similar but not exactly the same, and therefore
 185 the previous relations should be computed for all the nodes of the network. To
 186 avoid this problem, the computed standard deviation has been intentionally over-
 187 estimated in order to include as much nodes as possible. As a result, this overes-
 188 timation increases the time needed to converge to a correct solution in the Particle
 189 Filter. Moreover, this overestimation does not solve the problem of biased measure-
 190 ments that could produce nodes which RSSI/Distance relation differs significantly
 191 from the one of the nodes used for the calibration. However, in the experimental
 192 results, with 25 nodes, no divergence was observed in the estimation due to biased
 193 measurements.

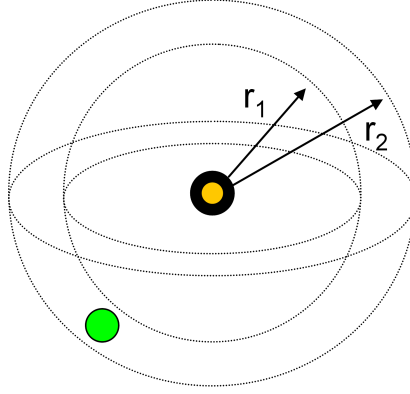


Fig. 3. Prior distribution. The initial samples are drawn from an uniform distribution over a spherical annulus. The inner (r_1) and outer (r_2) radius are a function of the estimated distance from the RSSI and its variance.

194 3.3 Updating

195 Once obtained, the functions $\mu(d_k)$ and $\sigma(d_k)$ are used online in the estimation process.
 196 Each time a new measure is received, the weights of the particles are updated
 197 considering the likelihood of the received data (lines 3, 4 and 5 of Algorithm 1).

198 The procedure is as follows. For each particle, the distance $d_k^{(i)} = \|\mathbf{x}_k^{(i)} - \mathbf{x}_k^r\|$ is
 199 obtained. From this distance, the mean and variance of the conditional distribution
 200 $p(\mathbf{z}_k | \mathbf{x}_k^{(i)})$ are obtained, so that $p(\mathbf{z}_k | \mathbf{x}_k^{(i)}) = \mathcal{N}(\mu(d_k^{(i)}), \sigma(d_k^{(i)}))$.

201 The probability of the actual RSSI value under this distribution is finally employed
 202 to update the weight of the particle $\omega_k^{(i)}$.

$$\omega_k^{(i)} = \frac{1}{\sigma(d_k^{(i)})\sqrt{2\pi}} \exp\left(-\frac{(RSSI_k - \mu(d_k^{(i)}))^2}{2\sigma(d_k^{(i)})^2}\right) \omega_{k-1}^{(i)} \quad (3)$$

203 After each update stage, the weights are normalized to have a sum equal to one
 204 (line 7 of Algorithm 1).

205 3.4 Initializing the filter. The prior model

206 The filter associated with a specific node is initiated when the first message is re-
 207 ceived in the mobile robot (it should be recalled that there is a separate filter per
 208 node). In this case, the *RSSI* distance functions of (2) are used inversely as in the
 209 estimation process. From the *RSSI* values, an initial distance is estimated, and also
 210 a corresponding variance on the distance.

211 The prior considered is then a uniform distribution on a spherical annulus, in which
 212 the inner and outer radius depend on the estimated mean and variance (see Fig.
 213 3). As the number of particles is limited, not all the messages received initiate the
 214 filter. Only when a *RSSI* value corresponding to a variance below a threshold is
 215 received, the filter is initiated, in order to have a good resolution (particles per vol-
 216 ume unit) with a limited number of particles. In the experiments show in this paper,
 217 this threshold has been set to $RSSI = 300$, that (according to Fig. 2) corresponds to
 218 distances shorter than 8 meters approximately.

219 3.5 Prediction

220 The nodes of the WSN are static, so the prediction step might be omitted (that is,
 221 with probability 1 each node is in the same position at time k and $k - 1$). However,
 222 as the resolution of particles over the state space is limited, a random move is added
 223 to the particles, in order to search locally over the area around the position of the
 224 previous time step. Therefore, the prediction model is:

$$p(\mathbf{x}_k | \mathbf{x}_{k-1}) = \mathcal{N}(\mathbf{x}_{k-1}, \Sigma_{k-1}) \quad (4)$$

225 The value of Σ depends on the spatial distribution of particles, mainly the density
 226 of particles per volume unit. The idea behind is to make the particles move around
 227 their position in order to approximately cover the half of the distance to the neigh-
 228 bor particles. This way, the particle will integrate the mean value of the weight
 229 associated to its area, not only the given position.

230 3.6 Resampling

231 In general, the mission of the resampling step is to spatially distribute the particles
 232 in order to increase the sampling of the posterior in the areas where the likelihood
 233 is high. Thus, the resampling step will duplicate particles with high weights and
 234 will eliminate those with very low weights.

235 If no resampling is carried out in the Particle Filter, it will slowly converge to
 236 an only one particle with a weight close to 1, while the rest of particles will be
 237 weighted by 0. There are two problems related with this behavior: first, the es-
 238 timated std. dev. becomes clearly sub-estimated, leading to the filter divergence,
 239 and, second, the spatial resolution of the filter is strongly limited by the number of
 240 particles, it leads to poor estimations. However, resampling reduces the diversity of
 241 the particle set [16].

242 Therefore, a resampling step (line 10 of Algorithm 1) is included in the filter to

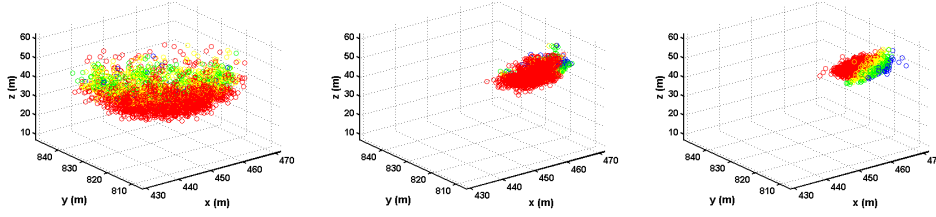


Fig. 4. An example of particles evolution at three stages. In the first one, it can be identified the sphere-like shape. As more messages are received, the particles concentrate into a unimodal distribution. The color represents the weight of the particle: Red between 0 and 0.25, Yellow between 0.25 and 0.5, Green between 0.5 and 0.75, Blue between 0.75 and 1.

243 increase the accuracy of the estimated position and to reduce the required particles.
 244 Two considerations are taken into account in this resampling step: first, resampling
 245 only takes place when the effective number of particles N_{eff} is below a threshold.
 246 The effective number is computed as follows:

$$N_{eff} = \left[\sum_{i=1}^L (\omega_k^{(i)})^2 \right]^{-1} \quad (5)$$

247 The threshold is set to the 10% of the number of particles, so $N_{th} = 0.1L$.

248 Second, the algorithm employed for sampling the particles space is a low variance
 249 sampler, particularly the algorithm described in [16] (p. 110). This method reduces
 250 the loss of diversity on the particle set in the resampling step.

251 3.7 Estimation of mean and standard deviation

252 The filter mean and standard deviation at time k can be computed as follows:

$$\mu_k = \sum_{i=1}^L [\mathbf{x}_k^{(i)} \omega_k^{(i)}], \quad \sigma_k^2 = \sum_{i=1}^L [(\mathbf{x}_k^{(i)} - \mu_k)^2 \omega_k^{(i)}] \quad (6)$$

253 One of the benefits of the Particle Filter is that allows to face multi-modal or non-
 254 parametric hypothesis. While the posterior distribution will depend on the measures
 255 during the transient state, the filter approximately converge to a Normal distribution
 256 in the position of the node. Figure 4 shows an example of the evolution of the
 257 particles for one node. It has been considered that the filter converges when σ_k
 258 is below a certain threshold during a period of time. In the implementation the
 259 threshold was set to $3m$ during at least 20 messages.

260 If the filter converges at time k_0 , the belief on the position of the node can be mod-

261 eled as a Normal distribution such as $\mathcal{N}(\mu_{k_0}, \sigma_{k_0})$. This allows switching to another
262 filter implementation like Extended Kalman Filter (EKF) or Extended Information
263 Filter (EIF) which will efficiently take into account the gaussian nature of the poste-
264 rior distribution. Next Section focus on the use of Information Filtering for refining
265 the initial estimation given by the Particle Filter approach.

266 4 DECENTRALIZED NODES POSITION REFINEMENT EMPLOYING 267 INFORMATION FILTERS

268 4.1 Description

269 Once the particle filter on the mobile robot has obtained a unimodal distribution for
270 the position of one node, the mean μ and covariance matrix Σ are transmitted to it.
271 Then, the node can locally refine its own position by using the information received
272 from the mobile robot and also from its neighbor nodes (which also have an initial
273 estimation of their positions). The messages exchanged among the nodes will be
274 always accompanied by the estimated position of the emitter. This information,
275 joined to the *RSSI* at the receiver, introduces a constraint on the possible positions
276 of emitter and receiver. By using measures from several neighbors or the mobile
277 robot, the position of the node can be further refined (see Fig. 5). Moreover, if
278 a node also maintains an estimation of the position of the neighbor nodes in its
279 communication range, this can be used for geographic routing of data.

280 The main issue for a decentralized estimation that runs on the nodes are the memory
281 restrictions that these nodes have, with a storage space of a few kilobytes.

282 4.2 Local filters

283 The information from neighbor nodes is integrated employing an Information Filter
284 (IF) [16]. The IF is a Gaussian Filter that employs the so-called *canonical represen-*
285 *tation* for the Gaussian distribution. The fundamental elements are the *information*
286 *matrix* $\Omega = \Sigma^{-1}$ and the *information vector* $\xi = \Sigma^{-1}\mu$. The properties of the Infor-
287 mation Filter allow easy decentralized data fusion at low computational cost thanks
288 to an efficient updating stage and to the naturally sparse characterization of the
289 information matrix respectively [16,5]. The sparseness of the information matrix
290 has been employed, for instance, in batch algorithms for the full SLAM problem,
291 as in [17]. Here, it will be employed to devise online algorithms for decentralized
292 estimations that are efficient in term of memory requirements.

293 In the most general case, each node maintains a local estimation of its position and

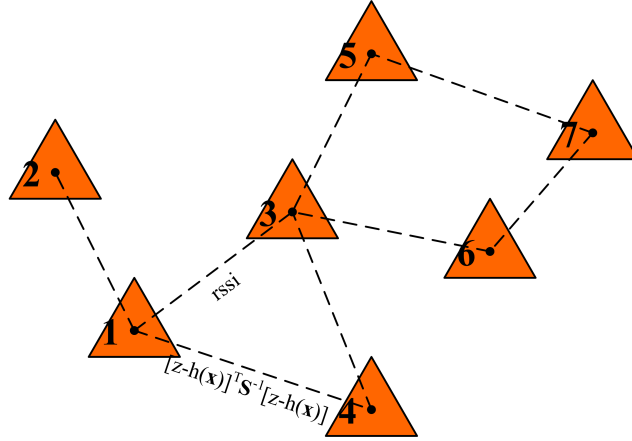


Fig. 5. The *RSSI* values received from neighbor nodes can be used as constraints over the positions of the different nodes of the network. These constraints are integrated by the nodes by using a decentralized Information Filter.

294 the position of its surrounding nodes. The state is maintained in information form.
 295 It is considered that nodes only have information about their own position at time
 296 0. Thus, for node 1 (denoted by ξ^1 and Ω^1), the initial state is given by:

$$\Omega_0^1 = \begin{pmatrix} \Omega_{11}^1 & \mathbf{0} & \dots & \mathbf{0} \\ \mathbf{0} & \mathbf{0} & \dots & \mathbf{0} \\ \vdots & \vdots & \ddots & \vdots \\ \mathbf{0} & \mathbf{0} & \dots & \mathbf{0} \end{pmatrix} \quad \xi_0^1 = \begin{pmatrix} \xi_1^1 \\ \mathbf{0} \\ \vdots \\ \mathbf{0} \end{pmatrix} \quad (7)$$

297 The state to be estimated (the node position and that of its neighbors) is static, so
 298 no prediction step is performed. Each node updates its map with the information
 299 received from its neighbors. In the general case, the received messages consists of
 300 the estimated position of the emitter. For instance, if the sender is node i , it sends its
 301 own position estimation as a pair ξ_i^i and Ω_{ii}^i . The receiver also computes the *RSSI*_{1i}
 302 value of the incoming message.

303 As shown in Section 3.2 and illustrated in Fig. 2, the measurement function $RSSI_t =$
 304 $h(\mathbf{x})$ is non-linear on the state, so the Extended Information Filter (EIF) is em-
 305 ployed. The updating equations for the EIF are:

$$\Omega_t^1 = \Omega_{t-1}^1 + \mathbf{M}_t^T \mathbf{S}_t^{-1} \mathbf{M}_t \quad (8)$$

$$\xi_t^1 = \xi_{t-1}^1 + \mathbf{M}_t^T \mathbf{S}_t^{-1} [\mathbf{z}_t - h(\mu_t) + \mathbf{M}_t \mu_t] \quad (9)$$

306 The updating equations of the EIF require an estimation of the variance σ_{rssi}^2 of

307 the received RSSI value in information form $\mathbf{S}_t^{-1} = \frac{1}{\sigma_{rssi}^2}$. This value is estimated
 308 by using the expression (2) evaluated at the mean distance between nodes. Also,
 309 the Jacobian \mathbf{M} of the measurement equation is required, which is obtained by
 310 linearizing the relation (2) around the current estimated mean of the state \mathbf{x} . The
 311 *RSSI* is a scalar value that depends on the distance between the two nodes $d_{1i} =$
 312 $\|\mathbf{x}_1 - \mathbf{x}_i\| = \sqrt{(\mathbf{x}_1 - \mathbf{x}_i)^T (\mathbf{x}_1 - \mathbf{x}_i)}$:

$$RSSI_{1i} = h(d_{1i}) = h(\|\mathbf{x}_1 - \mathbf{x}_i\|) \quad (10)$$

313 Then,

$$\mathbf{M} = \frac{\partial RSSI_{1i}}{\partial \mathbf{x}} = \frac{\partial h}{\partial d_{1i}} \frac{\partial d_{1i}}{\partial \mathbf{x}} = \underbrace{\frac{\partial h}{\partial d_{1i}} \frac{2}{2d_{1i}}}_M \left((\mathbf{x}_1 - \mathbf{x}_i)^T \mathbf{0} \cdots -(\mathbf{x}_1 - \mathbf{x}_i)^T \cdots \mathbf{0} \right) \quad (11)$$

314 where M is a scalar dependant on the mean distance between the nodes. It can be
 315 seen, from the form of \mathbf{M} , that the updating equations only affect the part of the
 316 information vector and matrix related to nodes 1 and i . Removing the time indexes,
 317 the final updating equations when receiving information from node i are:

$$\Omega_t^1 = \underbrace{\begin{pmatrix} \Omega_{11}^1 & \Omega_{1i}^1 \\ \Omega_{i1}^1 & \Omega_{ii}^1 \end{pmatrix}}_{fusion} + \begin{pmatrix} \mathbf{0} & \mathbf{0} \\ \mathbf{0} & \Omega_{ii}^i \end{pmatrix} + \frac{M^2}{\sigma_{rssi}^2} \begin{pmatrix} (\mathbf{x}_1 - \mathbf{x}_i)(\mathbf{x}_1 - \mathbf{x}_i)^T & -(\mathbf{x}_1 - \mathbf{x}_i)(\mathbf{x}_1 - \mathbf{x}_i)^T \\ -(\mathbf{x}_1 - \mathbf{x}_i)(\mathbf{x}_1 - \mathbf{x}_i)^T & (\mathbf{x}_1 - \mathbf{x}_i)(\mathbf{x}_1 - \mathbf{x}_i)^T \end{pmatrix} \quad (12)$$

$$\xi_t = \underbrace{\begin{pmatrix} \xi_1^1 \\ \xi_i^1 \end{pmatrix}}_{fusion} + \begin{pmatrix} \mathbf{0} \\ \xi_i^i \end{pmatrix} + \frac{M}{\sigma_{rssi}^2} \begin{pmatrix} \mathbf{x}_1 - \mathbf{x}_i \\ -(\mathbf{x}_1 - \mathbf{x}_i) \end{pmatrix} [RSSI - h(\mathbf{x}) + \mathbf{M}\mathbf{x}] \quad (13)$$

318 where \mathbf{x}_1 and \mathbf{x}_i are evaluated at the current means μ_1 and μ_i . As shown in [17], this
 319 estimation procedure is equivalent to obtaining the optimal position of the nodes
 320 under the restrictions on their positions \mathbf{x} induced by the *RSSI* values, which are of
 321 the form $[\mathbf{z}_t - h(\mathbf{x})]\mathbf{S}_t^{-1}[\mathbf{z}_t - h(\mathbf{x})]^T$ (see Fig. 5).

322 There are several issues to be pointed out. First, the application of all the previous
 323 equations maintains a sparse structure for the information matrix about the position

ξ_1	Ω_{11}	Ω_{12}	Ω_{13}	Ω_{14}
ξ_2	Ω_{21}	Ω_{22}		
ξ_3	Ω_{31}		Ω_{33}	
ξ_4	Ω_{41}			Ω_{44}

Fig. 6. Structure of the information matrix for the case considered.

324 of all the neighbor nodes that have communicated with node 1 (see Fig. 6). Then, it
325 can be seen that the memory requirements are linear with the number of neighbor
326 nodes. This is key issue for the implementation of the algorithm in sensor nodes.

327 Also, measurements induce relative relations, and therefore the state is not fully
328 observable. However, the nodes are already observed after the initial estimation
329 by using the particle filter. Also, the measurements from the robot, which position
330 uncertainty is independent from that of the nodes, allows anchoring the nodes to a
331 common reference frame. It is important to remark that the nodes do not maintain
332 an estimation of the position of the node on board the mobile robot. Thus, when
333 receiving information from the robot, the information about the robot position is
334 marginalized out.

335 Finally, the received local estimation about node i is fused with the current one.
336 As shown in eqs. (12) and (13), for a decentralized EIF, the fusion step is a simple
337 addition of the local information. This step can be modified to incorporate more
338 information, as described in the next section.

339 4.3 Decentralized estimation

340 The main idea is to estimate at each node the position of other nodes of the network
341 in a decentralized manner. The previous equations involve a decentralized fusion
342 of the marginal information ξ_{ii} and Ω_{ii} about the position of the emitter. However,
343 the emitter could include in the message its local estimation about the position of
344 all its surrounding nodes. This way, more information could be used for position
345 refinement in the fusion step. Also, each node would finally had knowledge about
346 the positions of all the nodes of the network.

347 The problem derived from this scheme is that the sparsity is lost (see Fig. 7). There-
348 fore, the storage requirements increases (which is the main limitation for this kind
349 of nodes), and the size of the message needed to transmit the information as well.

350 Besides, the updating equations require maintaining an estimation of the mean μ
351 of \mathbf{x} for the computation of the updating stage (12) and (13). This would require
352 to solve the system $\xi = \Omega\mu$. If the sparsity of the system is maintained, efficient

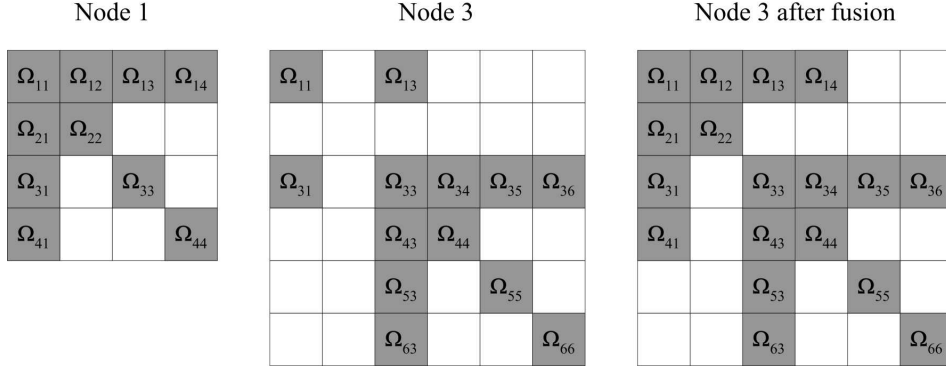


Fig. 7. Left and centre: local estimations of nodes 1 and 3 for the situation of Fig. 5. Right: estimation at node 3 after fusing all information from node 1. It can be seen that exchanging the full map leads to a higher density in the information matrix.

353 algorithms can be used.

354 The option considered here is to send with each message not only the marginal
 355 information about the emitter, but also its local estimation about the position of the
 356 receiver. This way, the fusion equations are changed by:

$$\Omega_t^1 = \begin{pmatrix} \Omega_{11}^1 & \Omega_{1i}^1 \\ \Omega_{i1}^1 & \Omega_{ii}^1 \end{pmatrix} + \begin{pmatrix} \Omega_{11}^i & \Omega_{1i}^i \\ \Omega_{i1}^i & \Omega_{ii}^i \end{pmatrix} \quad (14)$$

357 and:

$$\xi_t^1 = \begin{pmatrix} \xi_1^1 \\ \xi_i^1 \end{pmatrix} + \begin{pmatrix} \xi_1^i \\ \xi_i^i \end{pmatrix} \quad (15)$$

358 where the sums only affect the part of the state corresponding to nodes 1 and i , and
 359 thus maintain the structure of the information matrix. In order to do that, each time
 360 information is sent to a node, the marginal information about emitter and receiver
 361 is extracted. The marginal of a multivariate Gaussian can be computed in closed
 362 form [16]. In the particular case of matrices with the structure of Fig. 6, the compu-
 363 tation requirements only involve inversions of 3×3 matrices and local operations.
 364 For instance, marginalizing out the information about node 4 in that example only
 365 affects node 1 (see Fig. 8):

$$\begin{aligned} \bar{\Omega}_{11} &= \Omega_{11} - \Omega_{14}\Omega_{44}^{-1}\Omega_{41} \\ \bar{\xi}_1 &= \xi_1 - \Omega_{14}\Omega_{44}^{-1}\xi_4 \end{aligned} \quad (16)$$

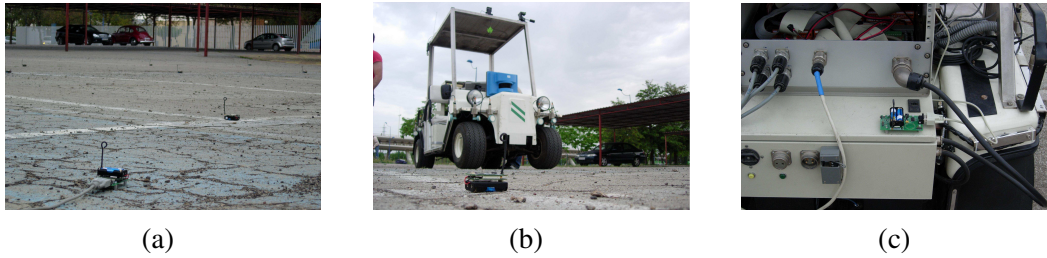


Fig. 9. Experiment setup. (a): 25 Mica2 nodes spread in the parking area of the University of Seville. (b): Romeo, the mobile robot used to interact with the network. (c): Node mounted on Romeo

383 5 EXPERIMENTAL RESULTS

384 This section details the results of an experimental setup conceived to test the above
 385 algorithms. A wireless sensor network composed of 25 Mica2 nodes was deployed
 386 in a parking area, see Fig. 9(a). The position of all the nodes were computed using
 387 a DGPS device in order to validate the algorithm estimations.

388 A ground robot (Romeo) is used to localize the nodes, see Fig. 9(b). Romeo is
 389 equipped with DGPS, gyroscope, compass and other navigation devices. Three
 390 computers onboard Romeo (one Pentium IV and two Pentium Mobile) allow com-
 391 plex data processing. In addition, one WSN node was mounted and connected to
 392 Romeo through a serial link cable, Fig. 9(c). The node runs a software that relays
 393 all received messages to Romeo.

394 The Particle Filter based localization has been implemented in C++ and runs on-
 395 board Romeo. The onboard software received all the messages from the WSN and
 396 the positioning information from the DGPS device. A filter with 4000 particles and
 397 non-prior information was implemented per node.

398 Figure 10 shows the evolution of the error in the estimated position for X, Y and
 399 Z axes for one node of the network. The error is computed as the distance between
 400 the estimation using the Particle Filter approach and the actual DGPS position of
 401 the node. The figure shows the estimated standard deviation per axis as well. It can
 402 be seen that the std. dev. is consistent with the error committed.

403 It is not possible to show the evolution of the error for all the nodes due to space
 404 restrictions. Instead, it is presented in Fig. 11 the mean error committed in the
 405 estimated position of the 25 nodes by using the Particle Filter approach. The figure
 406 shows the mean error of all the network after receiving x messages.

407 The Information Filter approach for position refinement is still not implemented
 408 inside the nodes, so that all the required data for testing the algorithm (*RSSI*, emitter
 409 and receiver) were extracted from the network through a gateway and stored in a
 410 file. It means that the experiments were carried out off-line but with actual data

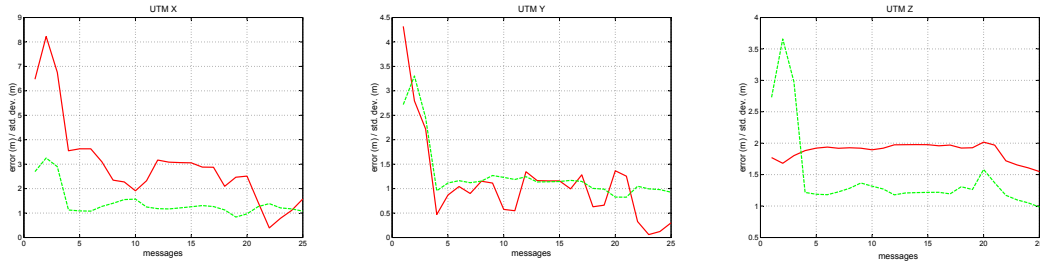


Fig. 10. Estimation error in meters computed as the distance between the DGPS position and the Particle Filter based estimation (red-solid). Standard deviation in meters obtained from the particles (green-dashed). The estimated distribution is consistent with the errors.

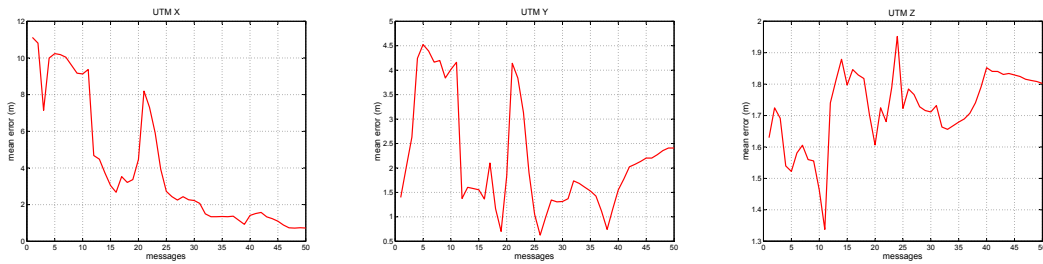


Fig. 11. The figures shown the mean error in meters committed after receiving x messages.

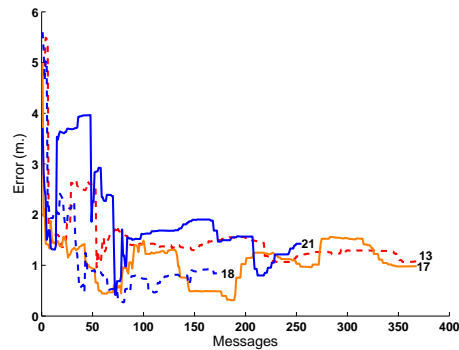


Fig. 12. Evolution of the error between the estimated position and actual position of several nodes employing the decentralized IF scheme.

411 from the network.

412 Figure 12 shows the correction on the error of the estimated position for several
 413 nodes. Figure 13 shows the estimated position for the two nodes compared to the
 414 actual ones.

415 6 CONCLUSIONS AND FUTURE WORK

416 The paper has shown a technique for estimating the position of the nodes of a WSN
 417 by using the received signal strength in a mobile robot and a distributed method

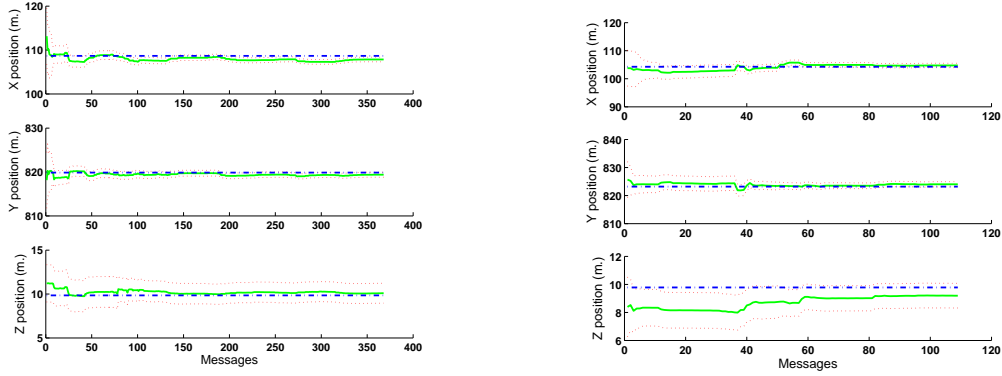


Fig. 13. Evolution of the estimated position for two different nodes by using the IF approach. Solid, estimated position. Dash-dot, position measured by DGPS. Depending on the distribution of the neighbor nodes, some coordinates are better resolved than others.

418 for position refinement using the normal data flow of the network. Both techniques
 419 have been tested in real conditions and the results showed their good feasibility.

420 The Particle Filter based localization has been tested online in a real robot. The
 421 needed computation to run the filters is low and the errors committed to the esti-
 422 mation are reasonable. The authors explored the implementation of this algorithm
 423 inside the nodes but the memory requirements for the particle storage, around 4k
 424 bytes, make it difficult given the usual memory restrictions in the nodes.

425 The decentralized scheme allows that improvements in part of the network propa-
 426 gates to others. Although this decentralized position refinement using the Informa-
 427 tion Filter has been tested offline, the results are promising. The low computation
 428 requirements needed to update the filter joint to a fixed state vector with three or
 429 four neighbors make possible the implementation inside the nodes. Next steps will
 430 consider this issue.

431 Certainly, some robot motions are much more convenient for the localization of
 432 the nodes than others. The inclusion of the network localization in the NRS path
 433 planning will be researched. Equation (12) allows to obtain an estimation of the in-
 434 formation gain (for instance as the expected difference of entropy of the probability
 435 distributions) for a given position of the robot and an expected value of the *RSSI*.
 436 Figure 14 shows the estimated information gain for different positions of a robot
 437 and a network of three nodes. This information gain can be used within greedy ex-
 438 ploration strategies to generate robot actions that will reduce the uncertainty in the
 439 estimated position of the nodes of the WSN.

440 Finally, in this paper the likelihood function that relates *RSSI* and distance was es-
 441 timated off-line and then maintained fixed. Improvements to re-estimate online the
 442 functions by using methods like Expectation-Maximization [10] will be researched.

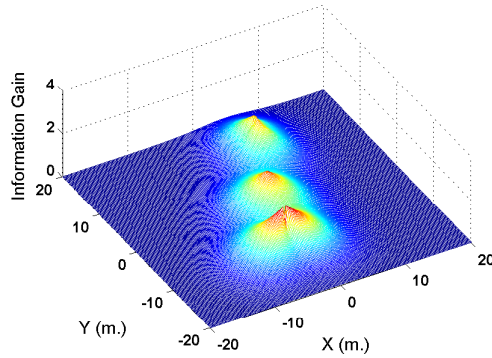


Fig. 14. Expected information gain for a network of three nodes at positions $(0,0)$, $(5,12)$ and $(-3,-10)$ and a mobile robot. The information gain is computed as the expected variation of the entropy of the distribution on the node position.

443 7 ACKNOWLEDGMENTS

444 The authors thank the help of Antidio Viguria for supporting part of the WSN
 445 experiments needed to validate the Particle Filter approach presented in this paper.
 446 The authors also thank the collaboration of the AWARE project team.

447 References

- 448 [1] A. Brooks, S. Williams, A. Makarenko, Automatic online localization of nodes in
 449 an active sensor network, in: Proc. IEEE Int. Conf. Robotics and Automation, New
 450 Orleans, 2004.
- 451 [2] N. Bulusu, J. Heidemann, D. Estrin, GPS-less low-cost outdoor localization for very
 452 small devices, *IEEE Personal Communications* 7 (5) (2000) 28–34.
- 453 [3] P. Dang, F. L. Lewis, D. O. Popa, Dynamic localization of air-ground wireless sensor
 454 networks, in: Proceeding of the 14th Mediterranean Conference on Control and
 455 Automation, 2006.
- 456 [4] A. Doucet, N. de Freitas, N. Gordon (eds.), *Sequential Monte Carlo Methods in
 457 Practice*, Springer-Verlag, 2001.
- 458 [5] R. Eustice, H. Singh, J. Leonard, Exactly Sparse Delayed-State Filters for View-Based
 459 SLAM, *IEEE Transactions on Robotics* 22 (6) (2006) 1100–1114.
- 460 [6] S. Grime, H. F. Durrant-Whyte, Data fusion in decentralized sensor networks, *Control
 461 Engineering Practice* 2 (5) (1994) 849–863.
- 462 [7] S. Julier, J. Uhlmann, A non-divergent estimation algorithm in the presence of
 463 unknown correlations, in: *Proceedings of the American Control Conference*, vol. 4,
 464 1997.

- 465 [8] S. Julier, J. Uhlmann, Using covariance intersection for SLAM, *Robotics and*
466 *Autonomous Systems* 55 (1) (2007) 3–20.
- 467 [9] R. Moses, D. Krishnamurthy, R. Patterson, A self-localization method for wireless
468 sensor networks, *EURASIP Journal on Applied Signal Processing* (4) (2003) 348–
469 358.
- 470 [10] R. Neal, G. Hinton, A view of the EM algorithm that justifies incremental, sparse, and
471 other variants, MIT Press, Cambridge, MA, USA, 1999, pp. 355–368.
- 472 [11] N. Patwari, A. O. Hero, Using proximity and quantized RSS for sensor localization
473 in wireless networks, in: *Proc. of the 2nd ACM international conference on Wireless*
474 *sensor networks and applications, WSNA 2003*, ACM Press, New York, NY, USA,
475 2003.
- 476 [12] V. Ramadurai, M. L. Sichitiu, Localization in wireless sensor networks: A probabilistic
477 approach, in: *Proceedings of the 2003 International Conference on Wireless Networks*
478 *(ICWN 2003)*, Las Vegas, NV, 2003.
- 479 [13] I. Rekleitis, D. Meger, G. Dudek, Simultaneous planning, localization, and mapping in
480 a camera sensor network, *Robotics and Autonomous Systems* 54 (11) (2006) 921–932.
- 481 [14] M. Sichitiu, V. Ramadurai, Localization of wireless sensor networks with a mobile
482 beacon, in: *Proc. of the IEEE International Conference on Mobile Ad-hoc and Sensor*
483 *Systems (MASS)*, 2004.
- 484 [15] M. Terwilliger, A. G. V. Bhuse, Z. H. Kamal, M. A. Salahuddin, A localization system
485 using wireless sensor networks: A comparison of two techniques, in: *Proc. of the*
486 *First Workshop on Positioning, Navigation and Communication*, Hannover, Germany,
487 2004.
- 488 [16] S. Thrun, W. Burgard, D. Fox, *Probabilistic Robotics*, The MIT Press, 2005.
- 489 [17] S. Thrun, M. Montemerlo, The Graph SLAM Algorithm with Applications to Large-
490 Scale Mapping of Urban Structures, *The International Journal of Robotics Research*
491 25 (5-6) (2006) 403–429.
- 492 [18] K. Whitehouse, D. Culler, Macro-calibration in sensor/actuator networks, *Mobile*
493 *Networks and Applications* 8 (4) (2003) 463–472.
- 494 [19] S. Yang, H. Cha, An empirical study of antenna characteristics toward rf-based
495 localization for iee 802.15.4 sensor nodes, in: *4th European conference on Wireless*
496 *Sensor Networks, EWSN 2007*, Delf, The Netherlands, 2007.